Protein kinase SnRK2 . 4 is a key regulator of aquaporins and root hydraulics in Arabidopsis

Zaigham Shahzad, Colette Tournaire-Roux, Matthieu Canut, Mattia Adamo, Jan Roeder, Lionel Verdoucq, Alexandre Martinière, Anna Amtmann, Véronique Santoni, Erwin Grill, et al.

the plant journal

SEB SOCIETY FOR EXPERIMENTAL BIOLOGY

The Plant Journal (2023) doi: 10.1111/tpj.16494

Protein kinase SnRK2.4 is a key regulator of aquaporins and root hydraulics in Arabidopsis

Zaigham Shahzad[1,†], Colette Tournaire-Roux[1], Matthieu Canut[2], Mattia Adamo[1], Jan Roeder[3], Lionel Verdoucq[1], Alexandre Martinière[1], Anna Amtmann[4], Véronique Santoni[1], Erwin Grill[3], Olivier Loudet[2] and Christophe Maurel[1,*]

[1]*Institute for Plant Sciences of Montpellier, University Montpellier, CNRS, INRAE, Institut Agro, Montpellier, France,*
[2]*Université Paris-Saclay, INRAE, AgroParisTech, Institut Jean-Pierre Bourgin (IJPB), 78000 Versailles, France,*
[3]*School of Life Sciences, Technical University Munich, 85354 Freising-Weihenstephan, Germany,*
[4]*Institute of Molecular, Cell and Systems Biology, College of Medical, Veterinary and Life Sciences, University of Glasgow, Bower Building, Glasgow G12 8QQ, UK*

Received 2 May 2023; revised 6 September 2023; accepted 14 September 2023.
*For correspondence (e-mail christophe.maurel@cnrs.fr).
[†]Present address: Department of Life Sciences, SBA School of Science and Engineering, Lahore University of Management Sciences, D.H.A. Lahore Cantt. 54792, Lahore, Pakistan

SUMMARY

Soil water uptake by roots is a key component of plant water homeostasis contributing to plant growth and survival under ever-changing environmental conditions. The water transport capacity of roots (root hydraulic conductivity; Lp_r) is mostly contributed by finely regulated Plasma membrane Intrinsic Protein (PIP) aquaporins. In this study, we used natural variation of Arabidopsis for the identification of quantitative trait loci (QTLs) contributing to Lp_r. Using recombinant lines from a biparental cross (Cvi-0 x Col-0), we show that the gene encoding class 2 Sucrose-Non-Fermenting Protein kinase 2.4 (SnRK2.4) in Col-0 contributes to >30% of Lp_r by enhancing aquaporin-dependent water transport. At variance with the inactive and possibly unstable Cvi-0 SnRK2.4 form, the Col-0 form interacts with and phosphorylates the prototypal PIP2;1 aquaporin at Ser121 and stimulates its water transport activity upon coexpression in *Xenopus* oocytes and yeast cells. Activation of PIP2;1 by Col-0 SnRK2.4 in yeast also requires its protein kinase activity and can be counteracted by clade A Protein Phosphatases 2C. SnRK2.4 shows all hallmarks to be part of core abscisic acid (ABA) signaling modules. Yet, long-term (>3 h) inhibition of Lp_r by ABA possibly involves a SnRK2.4-independent inhibition of PIP2;1. *SnRK2.4* also promotes stomatal aperture and ABA-induced inhibition of primary root growth. The study identifies a key component of Lp_r and sheds new light on the functional overlap and specificity of SnRK2.4 with respect to other ABA-dependent or independent SnRK2s.

Keywords: abscisic acid, aquaporin, cell signalling, natural variation, phosphorylation, plasma membrane, protein kinase, SnRK2, root, water transport.

INTRODUCTION

Plants have evolved numerous physio-morphological traits to maintain their water status and face adverse environmental conditions, including water deficit in the soil (drought) or the atmosphere (evaporative demand) (Zhu, 2016). These traits, which allow a continuous adjustment of water delivery throughout the plant for growth and transpiration, include stomatal opening and closing, cell osmotic adjustment, regulation of tissue water permeability (hydraulics) and, on the longer term, alteration of root system growth and architecture, and leaf area.

A critical role of roots in this context is uptake of soil water (Maurel & Nacry, 2020; Scharwies & Dinneny, 2019). This first requires radial transport of water across concentric root cell layers prior to loading into xylem vessels and axial transport to the plant aerial parts (Boursiac et al., 2022). Radial water transport occurs along cell wall continuities (apoplastic path) or from cell to cell, through plasmodesmadata (symplastic path), or across membranes (transcellular path). The latter path is dominated by the function and regulation of aquaporins of the Plasma membrane Intrinsic Protein (PIP) subclass (Chaumont & Tyerman, 2014; Maurel et al., 2015). Fine-tuning of their opening and closing and regulated expression at the plasma membrane provides multiple potentialities for rapid and reversible adjustment of root hydraulic conductivity (Lp_r) in response to numerous

environmental stimuli (*e.g.* water deficit, flooding, nutrient availability) or endogenous signals related to abiotic stress or plant defense (Chaumont & Tyerman, 2014; Maurel et al., 2015). For instance, the plant hormone abscisic acid (ABA), which accumulates during water deficit, salinity, heat, and cold stresses acts on aquaporin expression in numerous plant species and causes changes in whole root and root cell hydraulic conductivity (Fan et al., 2015; Hose et al., 2000; Mahdieh & Mostajeran, 2009; Olaetxea et al., 2015). Effects of ABA were stimulatory in most studies although ABA-dependent inhibitions of root hydraulics could be observed, depending on plant species and hormone concentration (discussed in Mahdieh & Mostajeran, 2009). In *Arabidopsis thaliana* guard cells, phosphorylation-dependent activation of *At*PIP2;1 by ABA mediates a dual hydraulic and signaling function of this hormone, thereby favoring stomata closure and water conservation (Grondin et al., 2015; Rodrigues et al., 2017).

ABA signaling is mediated by core functional modules comprising ABA-binding PYR/PYL/RCAR proteins acting in concert with clade A Protein Phosphatases 2C (PP2C) (Cutler et al., 2010; Raghavendra et al., 2010). In association with ABA, this complex releases the PP2C-dependent deactivation of class 2 Sucrose-Non-Fermenting Protein kinases (SnRK2s), including SnRK2.2, SnRK2.3 and SnRK2.6 (also known as OST1), which in turn activate various targets such as AREB transcription factors (Yoshida et al., 2010), membrane transport proteins (Brandt et al., 2012; Grondin et al., 2015) or miRNA processing components (Yan et al., 2017). While an ABA signaling pathway was initially reconstituted in vitro (Fujii et al., 2009), recent co-expression studies in yeast allowed to assemble a variety of core ABA signaling modules acting in concert with various SnRK2s to activate in an ABA-dependent or independent manner AREB transcription factors, which in turn enhance expression of a luciferase reporter (Ruschhaupt et al., 2019).

The SnRK2 gene family comprises ten members (SnRK2.1 to 10) in Arabidopsis (Kulik et al., 2011), further classified into three groups (I-III). SnRK2 protein kinases are key regulators of plant response to water deficit, as induced by drought or salt stress. Group II (SnRK2.7 and 8) and group III (SnRK2.2, 3 and 6) members are known to be responsive to ABA, showing weak and strong activation, respectively (Boudsocq et al., 2004). However, all SnRK2s can be activated by osmotic stress and, in addition, group I SnRK2s (SnRK2.1, 4 and 10) mediate responses to oxidative treatments (Boudsocq et al., 2004; McLoughlin et al., 2012; Kulik et al., 2012). Recent studies showed that group I SnRK2s interact with VARICOSE, an mRNA decapping activator, and VARICOSE RELATED to regulate mRNA decay of numerous osmotic and salt stress-responsive genes thereby controlling root development and response to salt (Kawa et al., 2020; Soma et al., 2017). SnRK2s are themselves phosphorylated by osmotic-stress-activated Raf-like protein kinases which act as SnRK2 activators (Katsuta et al., 2020; Lin et al., 2020; Soma et al., 2020; Takahashi et al., 2020).

Natural genetic variation offers a great opportunity to discover adaptive mechanisms that fine-tune plant response to their environment and to identify genetic variants that can be used in plant improvement. As for numerous other traits, Arabidopsis exhibits marked within-species variation for drought sensitivity, phytohormone accumulation and/or signaling, and root hydraulics (Weigel, 2012). In the present work, we pursued studies on natural variation for root water permeability (root hydraulic conductivity, Lp_r) in Arabidopsis (Shahzad et al., 2016; Sutka et al., 2011; Tang et al., 2018). To identify genetic factors relevant to this trait, we explored recombinant inbred lines (RILs) developed by crossing two accessions, Col-0 and Cvi-0. Multiple quantitative trait loci (QTLs) controlling Lp_r under standard growth conditions were detected in this population. Alternative genotypes harboring either a Col-0 or Cvi-0 allele at one QTL displayed remarkable (>30%) variation for Lp_r. Positional cloning of the corresponding causative gene identified *SnRK2.4*. The overall work unravels *SnRK2.4* as a major control of root water transport through modulation of aquaporin function.

RESULTS

Identification of Lp_r QTLs in a Cvi-0 × Col-0 population.

A recombinant inbred line (RIL) population obtained by crossing the Col-0 and Cvi-0 accessions was grown under standard conditions and phenotyped for root hydraulics (Lp_r; root hydraulic conductance: *Lo*), plant growth (shoot and root dry weight) and development (bolting time). Plant growth and development traits were mapped to check for possible pleiotropic effects on root hydraulics. As previously reported for a Bur-0 x Col-0 RIL population (Shahzad et al., 2016), the Cvi-0 x Col-0 population showed transgressive segregation for all traits (Figure S1). Estimated heritability (h^2) varied from 0.24 to 0.39 (Table S1). Linkage mapping using Lp_r data identified three QTLs (Figure 1A), on the top of chromosome (Chr) 1 (Lprt18), bottom of Chr 2 (Lprb28), and bottom of Chr 5 (Lprb58). The two major Lp_r QTLs, Lprt18 and Lprb58, are positively contributed by Col-0 and Cvi-0 alleles, respectively. They were each confirmed using nearly isogenic lines of Heterogeneous Inbred Family (HIF)-type, fixed for either Col-0 or Cvi-0 allele: HIF046 for Lprt18 and HIF062 for Lprb58 (Figure 1B; Figure S2). HIF046-Col-0 showed a higher Lp_r than HIF046-Cvi-0 by 33.2% (Figure 1B), whereas HIF062-Col-0 showed a lower Lp_r than HIF062-Cvi-0 by 28.9% (Figure S2). While Lprb58 will be the object of future studies, we focused on Lprt18 in the present work. Upon treatment with sodium azide (NaN_3), a pharmacological inhibitor of aquaporins (Tournaire-Roux et al., 2003), HIF046 plants harboring Cvi-0 or Col-0 alleles exhibited similar, strongly reduced Lp_r

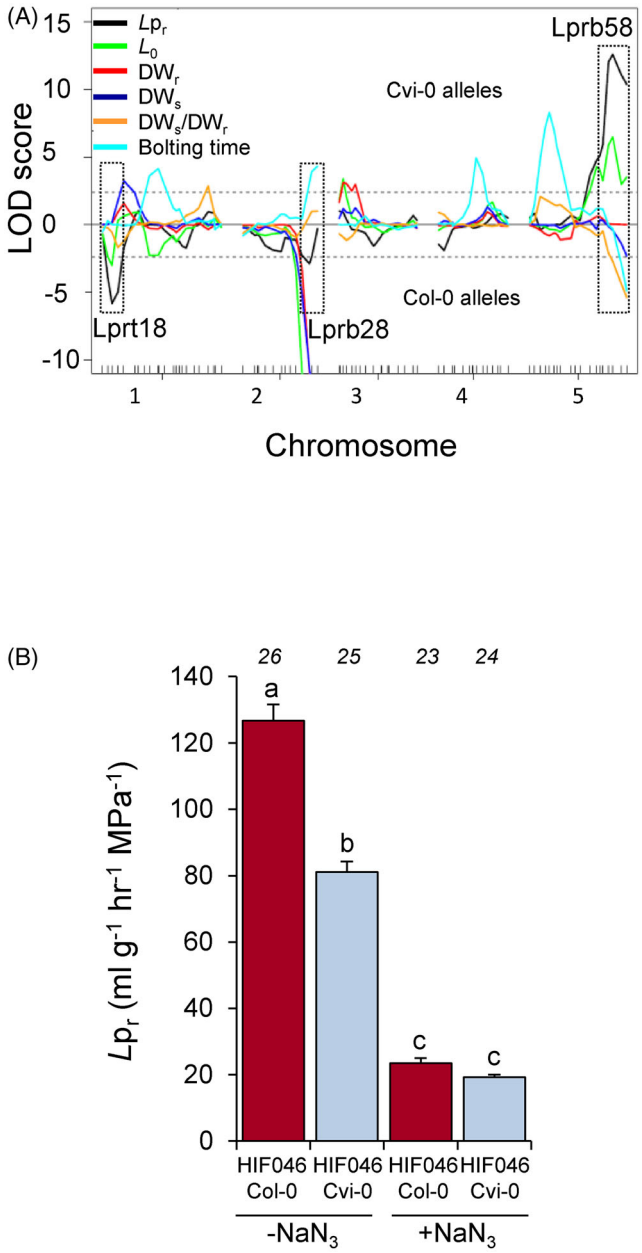

Figure 1. The Lprt18 QTL contributes to the natural variation of Lp_r.
(A) QTL map for root hydraulics (Lp_r, L_0), root and shoot growth (DW_r, DW_s, and DW_s/DW_r), and bolting time obtained by multiple QTL mapping in a Cvi-0 x Col-0 RIL population. A LOD threshold of 2.5 was obtained from permutation. Positive and negative LOD scores represent a positive contribution of Cvi-0 and Col-0 parental alleles, respectively. The Lp_r QTLs are indicated using dotted rectangles.
(B) Lp_r of HIF046-Cvi-0 and HIF046-Col-0 lines in the absence or presence of NaN_3. Mean values (±SE) from the number of individual plants indicated on the top.

(Figure 1B). The overall data show that the Col-0 allele at Lprt18 confers an enhanced Lp_r due to a higher aquaporin functionality.

SnRK2.4 underlies the natural variation of Lp_r conferred by Lprt18.

HIF046 was heterozygous for a region of more than 5 Mb (Figure 2A). To reduce the QTL interval, fine mapping was performed by selecting recombinant HIFs (rHIFs) from a selfed heterozygous individual of HIF046 and by extensively geno- and pheno-typing the rHIFs in a progeny testing procedure. In total, 12 rHIFs helped to restrain the QTL to a ~ 50 kb region harboring 14 genes (Figures 2A,B). DNA sequence comparison of the restrained QTL interval between Col-0 and Cvi-0 (The 1001 Genomes Consortium, 2016) revealed the existence of numerous polymorphisms between the two accessions (Figure 2B). However, the only polymorphism that causes a change in protein

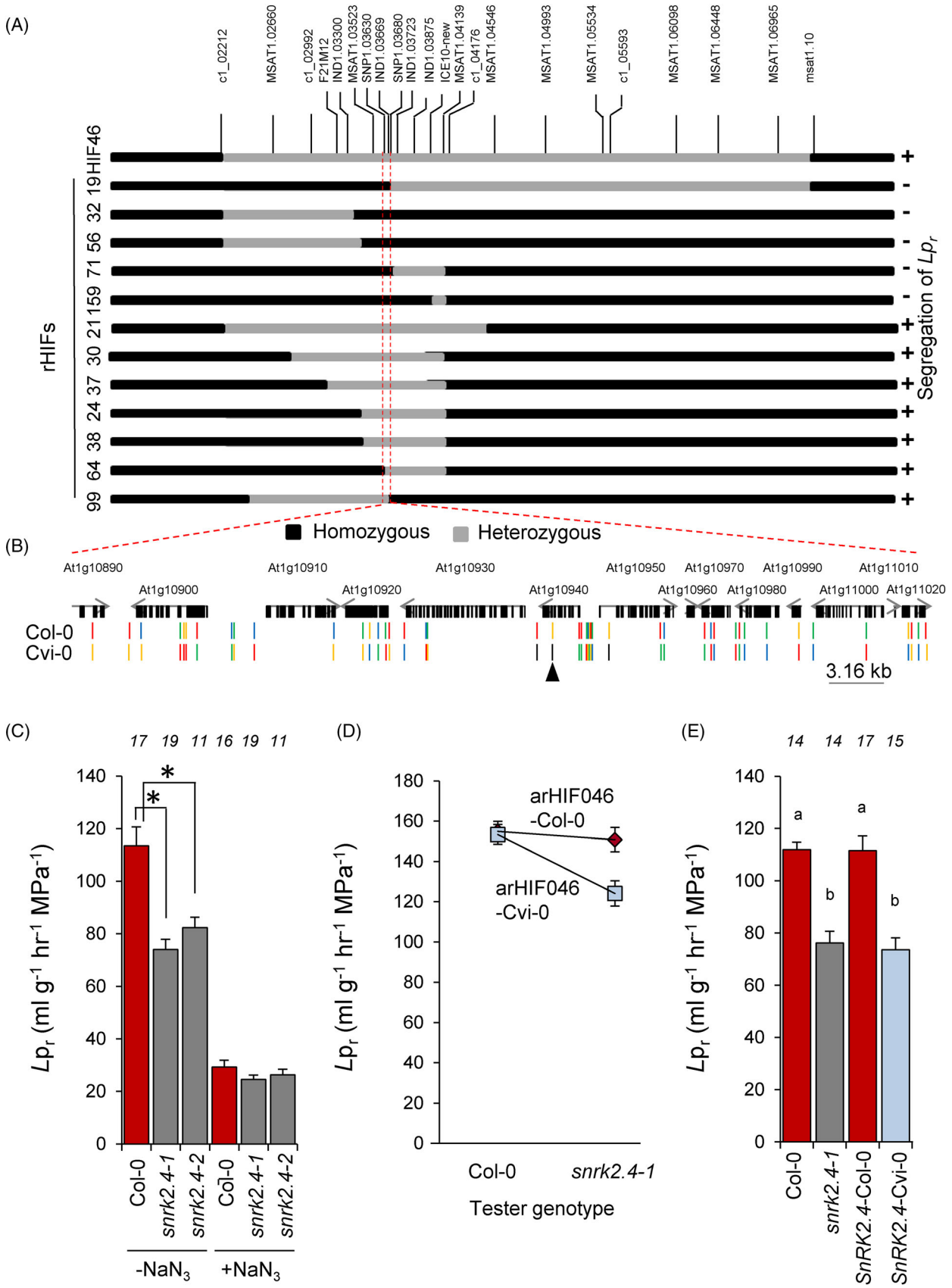

Figure 2. *SnRK2.4* underlies the root hydraulic Lprt18 QTL.
(A) Genetic structure of recombinant heterogeneous inbred families (rHIFs) used to fine map Lprt18. Heterozygous and homozygous regions are represented by gray and black bars, respectively. Genetic markers are listed at the top of the map. Phenotypic results for segregation (+) or lack of segregation (–) of Lp_r phenotype (similar to original HIF046) are indicated for each rHIF.
(B) Enlarged genomic region between SNP1.03630 and SNP1.03680 markers. The genes annotated in the fine-mapped candidate interval and the nucleotidic polymorphisms between Cvi-0 and Col-0 are indicated. Red, orange, green, blue, and black ticks represent adenine, thymine, guanine, cytosine, and indel, respectively. The indel polymorphism at At1g10940 (*SnRK2.4*) leading to a stop codon in the Cvi-0 coding DNA sequence is indicated by a black triangle.
(C) Lp_r of Col-0 and *snrk2.4* plants in the absence or presence of NaN_3. Data (mean ± SE) from the indicated number (*n*) of plants.
(D) Quantitative complementation of Lprt18. The graph shows the Lp_r of F1 allelic combinations obtained after crosses of either arHIF046-Col-0 or arHIF046-Cvi-0 with Col-0 or *snrk2.4-1*. The Lprt18 x *snrk2.4* genotype interaction term is significant at $P < 0.05$ (Two-way ANOVA) ($n = 29$–30).
(E) Lp_r of Col-0, *snrk2.4-1*, and *snrk2.4-1* lines expressing Col-0 or Cvi-0 *SnRK2.4* alleles. Same conventions as in (C).

sequence was present in the coding DNA sequence (CDS) of *At1g10940* (*SnRK2.4*). A single nucleotide deletion in the CDS of Cvi-0 SnRK2.4 leads, with respect to Col-0, to a frameshift and insertion of a premature stop codon that results in partial truncation of the protein kinase domain (Figure 2B; Figure S3). This polymorphism was also confirmed in the alternative genotypes of HIF046 (Figure S3). Based on this dramatic change in Cvi-0, we considered *SnRK2.4* as a potential candidate gene for Lprt18. Two independent knock-out mutant lines of *SnRK2.4* in Col-0 (*snrk2.4-1*, *snrk2.4-2)* (McLoughlin et al., 2012), were phenotyped for Lp_r. Consistent with the QTL effects, *snrk2.4* plants exhibited >30% lower Lp_r than Col-0 (Figure 2C); this phenotype is primarily due to a reduction in aquaporin activity, as revealed by a NaN_3 treatment.

To validate that *SnRK2.4* underlies Lprt18, we performed two distinct complementation tests. For quantitative complementation, advanced rHIFs segregating for Col-0 or Cvi-0 alleles within a region of about 50 kb around *SnRK2.4* were crossed to either *snrk2.4-1* or its wild-type background (Col-0), and the resulting 4 hybrid allelic combinations were phenotyped for Lp_r. A significant interaction between the QTL allele and the *SnRK2.4* allele was found, with higher Lp_r conferred by the Col-0 allele (Figure 2D). Molecular complementation of *snrk2.4-1* was also performed by introducing genomic regions carrying Col-0 or Cvi-0 *SnRK2.4* alleles using *Agrobacterium*-mediated transformation. Expression of the *SnRK2.4* transgenes was analyzed using qRT-PCR in independent transgenic lines (Figure S4a). Overall, the introduction of Col-0 *SnRK2.4* but not Cvi-0 *SnRK2.4* was able to complement the reduced Lp_r phenotype of *snrk2.4-1* (Figure 2E; Figure S4b). These complementation tests establish that variation at *SnRK2.4* explains the Lp_r phenotype segregating with Lprt18. Cvi-0 *SnRK2.4* appears as a non-functional allele, probably due to the insertion of a premature stop codon in its CDS (Figure S3).

SnRK2.4 does not alter the expression of PIP aquaporins in the plant but can phosphorylate their first cytoplasmic loop.

To address the mode of action of *SnRK2.4* on Lp_r and aquaporin activity, we investigated various regulatory levels of aquaporin expression. Comparative qRT-PCR and ELISA assays did not reveal any difference between Col-0 and *snrk2.4-1* or *snrk2.4-2* plants in the abundance of each of the 13 *PIP* mRNAs nor in protein accumulation of members of the PIP1 (PIP1;1 to PIP1;4) or PIP2 (PIP2;1 to PIP2;3) subfamilies, respectively (Figures S5a,b). PIP2;1 has previously been used as a prototypal isoform for studying the modes of PIP regulation (Li et al., 2011; Prak et al., 2008; Qing et al., 2016; Wudick et al., 2015). Introduction of a 35S::RFP-PIP2;1 construct in Col-0 and *snrk2.4-1* yielded similar fluorescence cellular patterns (Figures S5c,d) and similar fluorescence intensity at the cell surface (Figure S5e) between genotypes, indicating that SnRK2.4 does not interfere with the main localization and abundance of RFP-PIP2;1 at the plasma membrane. This lack of effects of *SnRK2.4* on PIP mRNA/protein abundance and sub-cellular localization prompted us to investigate the direct impact of SnRK2.4 on aquaporin phosphorylation, and aquaporin gating thereof (Maurel et al., 2015). Recombinant GST-tagged allelic forms of Col-0 and Cvi-0 SnRK2.4 were produced in *Escherichia coli* (Figure S6) and tested for their ability to phosphorylate PIP2;1 peptides *in vitro*. We opted for peptides corresponding to the first cytoplasmic loop (loop *B*) or the C-terminus domain of the protein, since these regions harbor well-described phosphorylation sites at Ser-121 and Ser-280/Ser-283, respectively (Grondin et al., 2015; Prak et al., 2008). Whereas C-terminal phosphorylation sites were not recognized, a strong phosphorylation activity was observed, specifically when Col-0 *SnRK2.4* was incubated with the PIP2;1 loop *B* peptide (Figure 3). These results conform to the substrate specificity of SnRK2.6 (OST1), a SnRK2.4 homolog previously shown to phosphorylate PIP2;1 at Ser121 (Grondin et al., 2015). They also support the idea that the Cvi-0 SnRK2.4 allelic form is functionally inactive (Figure 3).

Functional SnRK2.4 stimulates PIP2;1 water transport activity

To establish the effects of SnRK2.4 on PIP2;1 function, we used *Xenopus* oocytes and co-expressed a construct containing PIP2;1 fused to a C-terminal YFP half (YFP^C-PIP2;1) together with another construct containing SnRK2.4 fused to the complementary N-terminal half (YFP^N-SnRK2.4).

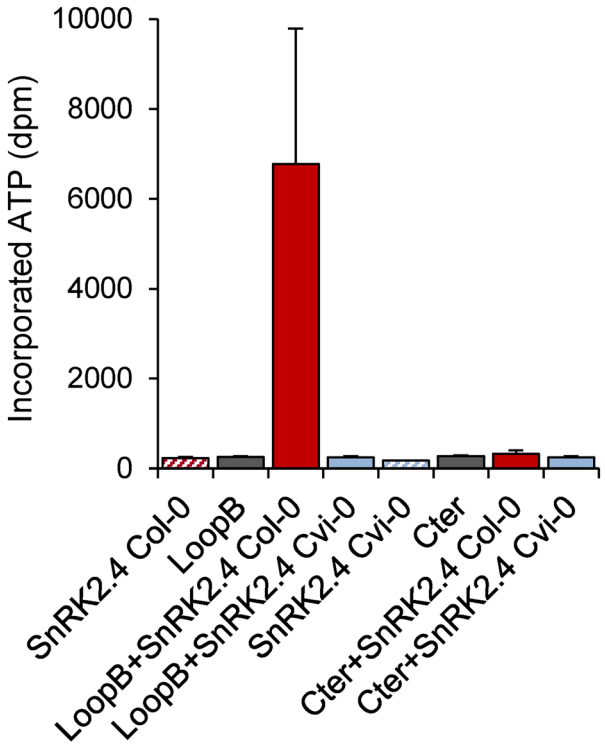

Figure 3. The Col-0 form of SnRK2.4 phosphorylates PIP2;1 at Ser-121.
In vitro phosphorylation of PIP2;1 peptides by recombinant SnRK2.4 forms from Col-0 or Cvi-0. Two peptides corresponding to the loop *B* and C-terminus (C-ter) of PIP2;1 were tested as substrates. Average (± SE) of incorporated ATP in these peptides is shown (n = 9).

Again, both Col-0 or Cvi-0 allelic forms of SnRK2.4 were investigated. These constructs, which permit Bimolecular Fluorescence Complementation (BiFC) assays, revealed that PIP2;1 interacts with Col-0 SnRK2.4 (Figures 4A,B), with a slightly lesser intensity than in PIP2;1 self-interactions, which generate well-described aquaporin homotetramers (Yoo et al., 2016). In contrast, no bimolecular interaction was detected between PIP2;1 and Cvi-0 SnRK2.4 (Figures 4A,B), which could partly be due to poor expression or instability of this truncated protein in oocytes (Figure 4C). Consistent with these observations, oocytes co-expressing YFP^C-PIP2;1 and Col-0 YFP^N-SnRK2.4 exhibited a higher water permeability (P_f) than oocytes co-expressing YFP^C-PIP2;1 and Cvi-0 YFP^N-SnRK2.4 (Figure 4D). Considering the latter oocytes as negative controls, the results suggest that Col-0 SnRK2.4 can stimulate PIP aquaporin activity in oocytes.

To further establish the activating role of SnRK2.4 and the contribution of its kinase activity, we used a yeast expression system and measured water transport using stopped-flow spectrophotometry. In this system, expression of PIP2;1 increased the osmotic water permeability (P_f) of isolated spheroplasts by about 10-fold with respect to a vector-transformed strain (Figure 5A). Co-expression of Col-0 SnRK2.4 with PIP2;1 further enhanced P_f by 40% without altering the overall expression level of PIP2;1 (ELISA assays on whole yeast extracts (in a.u. ± SE, n = 17): PIP2;1: 38.37 ± 1.86; PIP2;1 + SnRK2.4: 40.35 ± 1.79). Consistent with oocyte expression experiments, these data show that Col-0 SnRK2.4 activates PIP2;1 water transport activity. Furthermore, we used growth assays in yeast to monitor the capacity of PIP2;1 to transport hydrogen peroxide (H_2O_2). The enhanced sensitivity of yeast cells to 0.2 mM H_2O_2 observed upon expression of PIP2;1 was used as an easy, semi-quantitative readout of its activity (Figure 5B). In addition, GFP-SnRK2.4 fusions indicated that the Col-0 and Cvi-0 SnRK2.4 isoforms showed similar expression levels, mostly in the yeast cell cytoplasm (Figure S7). Yeast cells co-expressing Col-0 SnRK2.4 but not Cvi-0 SnRK2.4 with PIP2;1 displayed relatively higher sensitivity to H_2O_2 than PIP2;1 expressing cells. This assay confirms that Col-0 SnRK2.4 enhances PIP2;1 activity. Furthermore, the effects of Col-0 SnRK2.4 on stimulating PIP2;1 activity were abolished by a point mutation (D123A) in its catalytic site (Figure 5B). They also were counteracted by co-expression with the ABI1 PP2C but not its null D177A mutant (Figure 5B). Similar to ABI1, all 8 other members of the clade A PP2C family, except AHG1, were able to counteract the enhanced sensitivity to H_2O_2 of yeast cells co-expressing Col-0 SnRK2.4 with PIP2;1 (Figure S8). The overall data are interpreted to mean that the SnRK2.4 protein kinase activity, which can be inhibited upon co-expression with PP2Cs (Ruschhaupt et al., 2019), is required for PIP2;1 activation in yeast.

We conclude that SnRK2.4 can activate PIP2;1 likely through phosphorylation of loop *B*. The corresponding site is well conserved in PIPs and plays a general role in gating (Törnroth-Horsefield et al., 2006) thereby controlling water

Figure 4. The Col-0 form of SnRK2.4 stimulates PIP2;1 activity upon co-expression in *Xenopus* oocytes.
(A, B) BiFC analysis of interactions between PIP2;1 and SnRK2.4. Representative fluorescent images of oocytes expressing the indicated constructs (A) and a bar graph (B) of corresponding mean fluorescence are shown (n = 22–39 oocytes).
(C) Expression analysis of BiFC constructs in *Xenopus* oocytes. The figure shows a Coomassie stain (upper panel) and corresponding Western blot analysis using an anti-YFPn antibody (lower panel) of extracts from oocytes injected with cRNAs encoding the indicated constructs. NI: non injected. Red arrow heads in the second, third and fourth lanes indicate the detection at expected molecular weight of YFPn (21 kDa), YFPn-SnRK2.4 Col-0 (62 kDa), and YFPn-SnRK2.4 Cvi-0 (50.5 kDa), respectively. The upper band immunodetected at ~65 kDa and present in all lanes is thought to be unspecific.
(D) Mean (± SE) water permeability (P_f) of oocytes expressing the indicated BiFC constructs. n = 8–67.
In all experiments, cells were injected, as indicated, with 1 ng YFPc-PIP2;1 cRNA and/or 2.5 ng YFPn-SnRK2.4 (Col-0 or Cvi-0) cRNA.

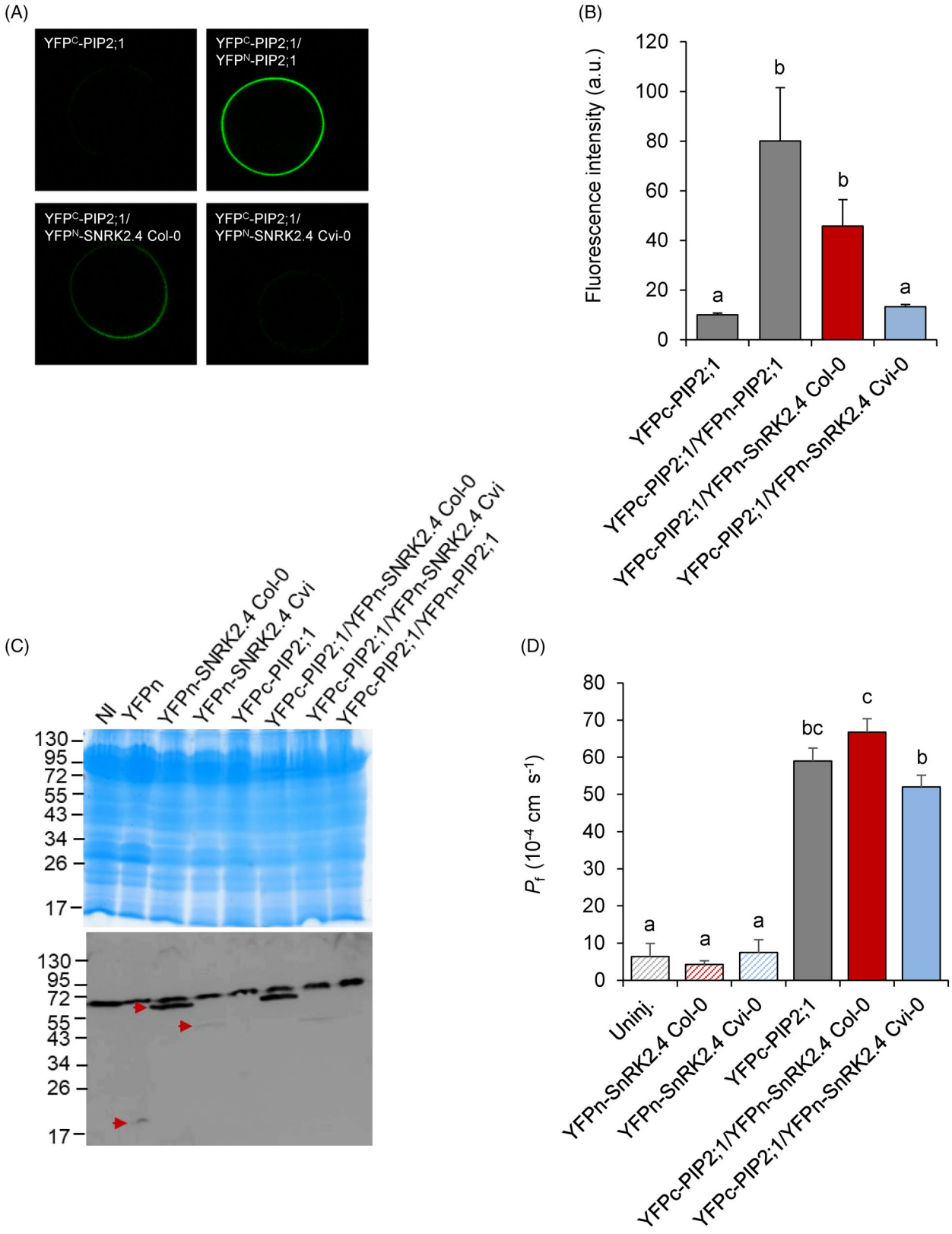

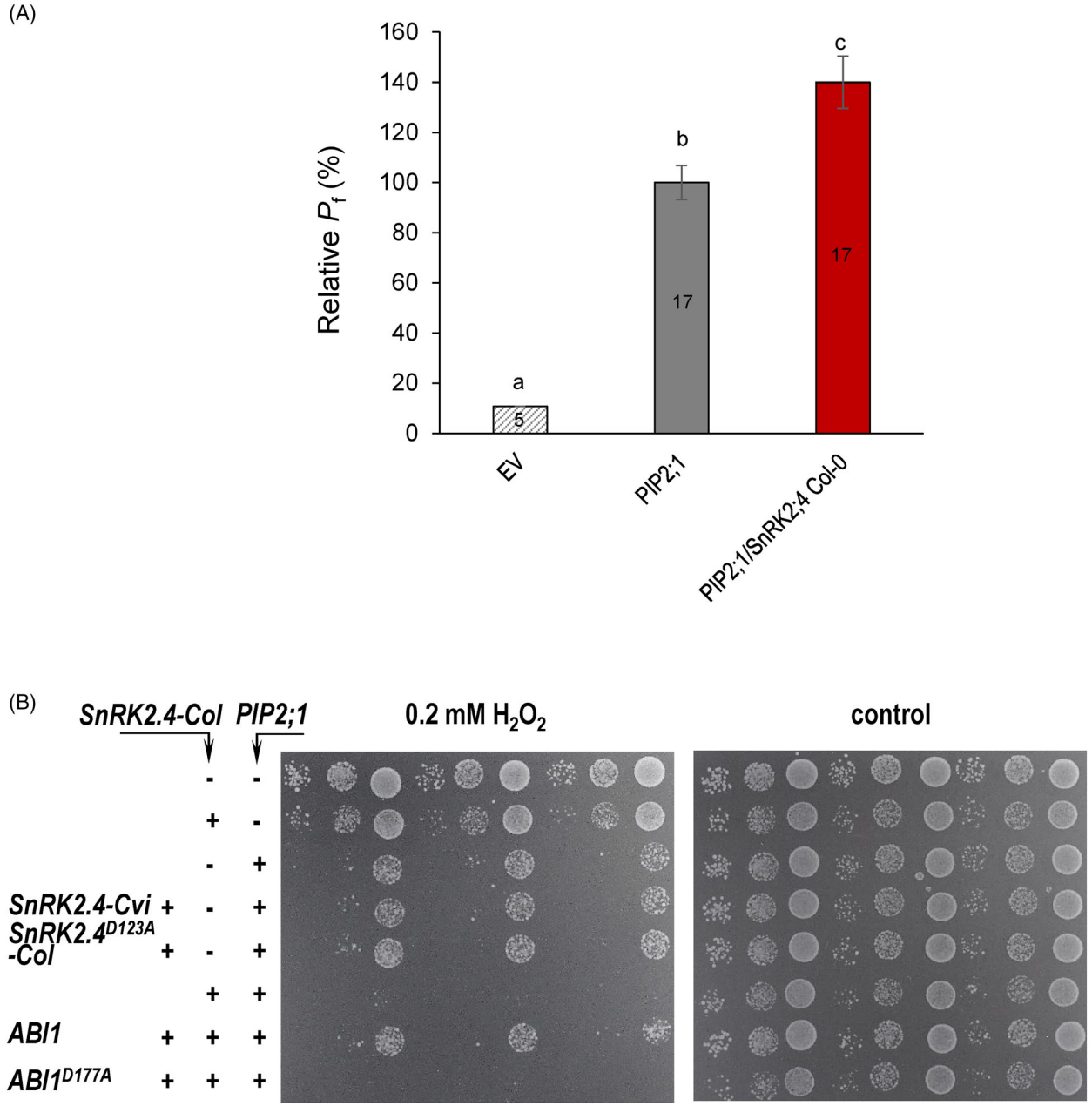

Figure 5. The protein kinase activity of SnRK2.4 is required to stimulate PIP2;1 activity upon co-expression in yeast.
(A) Yeast spheroplast water permeability (P_f) was determined by stopped-flow spectrophotometry (see Materials and methods). The figure shows the relative P_f values (means ± SE) of control yeasts (EV) or yeasts co-expressing SnRK2.4 Col-0 and PIP2;1 (red) with respect to yeasts expressing PIP2;1 alone (gray). Measurements were made in triplicate for every biological repeat (single yeast culture), the number of such repeats being shown in the figure.
(B) Growth assay of yeast lines expressing different *SnRK2.4* alleles, *PIP2;1*, and the PP2C *ABI1* for enhanced sensitivity towards H_2O_2. The expression of the catalytically active Col-0 allele and PIP2;1 is marked by the plus sign. Yeast expressing the Cvi-0 allele, ABI1, and functional inactive forms of SnRK2.4 and ABI1 with the mutation D123A and D177A in the catalytic domain, respectively, are indicated. Yeast cultures were grown to comparable cell densities and serial ten-fold dilutions were spotted on solidified medium in the presence and absence (control) of 0.2 mM H_2O_2. Growth of three independent transformants per combination was assessed after 2 days at 30°C.

or H_2O_2 transport (Lu et al., 2022). Notably, the *in vitro* phosphorylation assay, together with functional expression in oocytes and yeast matches the capacity of Col-0 SnRK2.4 to stimulate Lp_r in plants under resting conditions, whereas Cvi-0 SnRK2.4 does not.

Effects of exogenous ABA on Lp_r and role of PIP2;1.

SnRK2.4 is commonly described as an osmotic and salt-stress-induced protein kinase (Kawa et al., 2020; McLoughlin et al., 2012; Soma et al., 2017). Although responsiveness

of SnRK2.4 to ABA had not been anticipated by earlier activation studies (Boudsocq et al., 2004), recent data based on yeast expression (Ruschhaupt et al., 2019) indicate that SnRK2.4 may be involved in ABA-dependent signaling. These observations prompted us to characterize the responsiveness of Arabidopsis root hydraulics to both salt and ABA. In initial experiments with HIF046, a significant reduction of Lp_r was induced after treatment with a high exogenous ABA concentration (1 μM for 3 h) of HIF046-Col-0 (−30.7 ± 3.3%) but not HIF046-Cvi-0 (−12.1 ± 6.2%) plants (Figure S9). By contrast, HIF046-Col-0 and HIF046-Cvi-0 exhibited a similar inhibition of Lp_r by salt (150 mM NaCl), by −65.5 ± 2.7% and − 68.7 ± 1.7%, respectively (Figure S9). We therefore investigated in closer detail the effects of ABA on Col-0 and *snrk2.4-1* roots. Exogenous application of ABA resulted in a progressive inhibition of Lp_r in Col-0 which was visible after 3 h (−28%) and reached −51% after 7 h (Figure 6A). By contrast, Lp_r of *snrk2.4-1* plants or *snrk2.4-1* plants complemented with Cvi-0 SnRK2.4 remained unchanged during the first 3 h of ABA treatment (Figure 6A; Figure S10). After this time point, *snrk2.4-1* plants showed a tendency to progressive inhibition of Lp_r, with absolute values similar to those recorded in Col-0 (Figure 6A).

These data suggest that the pool of aquaporins that are activated by SnRK2.4 in roots under resting conditions is targeted during early inhibition of Lp_r by exogenous ABA. On a longer-term (>3 h), the hormone targets additional aquaporin pools active in both Col-0 and *snrk2.4* plants. To determine the PIP isoforms contributing to Lp_r and targeted by ABA-induced inhibition, we used a quintuple *pip* mutant (*pip2;1 pip2;2 pip2;4 pip2;6 pip2;7*: Quint) and the same genotype but complemented using a *PIP2;1* construct (Comp). When grown under control conditions, Quint plants showed, with respect to Col-0, a dramatically reduced Lp_r (−65%). In addition, Quint Lp_r was insensitive to inhibition after plant exposure to 1 μM ABA for 5 h. Under resting conditions, the Comp genotype showed a partial restauration of Lp_r that allowed, with respect to Quint, to monitor PIP2;1 activity. The Lp_r of Comp was significantly reduced after 5 h in the presence of ABA, demonstrating that ABA inhibits PIP2;1 activity.

Whole plant phenotypes

Expression in transgenic plants of a promSnRK2.4:: SnRK2.4-YFP reporter gene (McLoughlin et al., 2012) revealed that *SnRK2.4* is expressed in both roots and shoots, suggesting a role in tissue hydraulic regulation and/or ABA responses throughout the plant (Figures S11a–e). A typical organ response to ABA is primary root growth inhibition. When in vitro grown seedlings were treated with 25 μM ABA for 7 days, this inhibition was more pronounced in Col-0 (~62%) than in *snrk2.4-1* (~54%) (Figure 7A; Figure S11f). In this assay, the mutant root

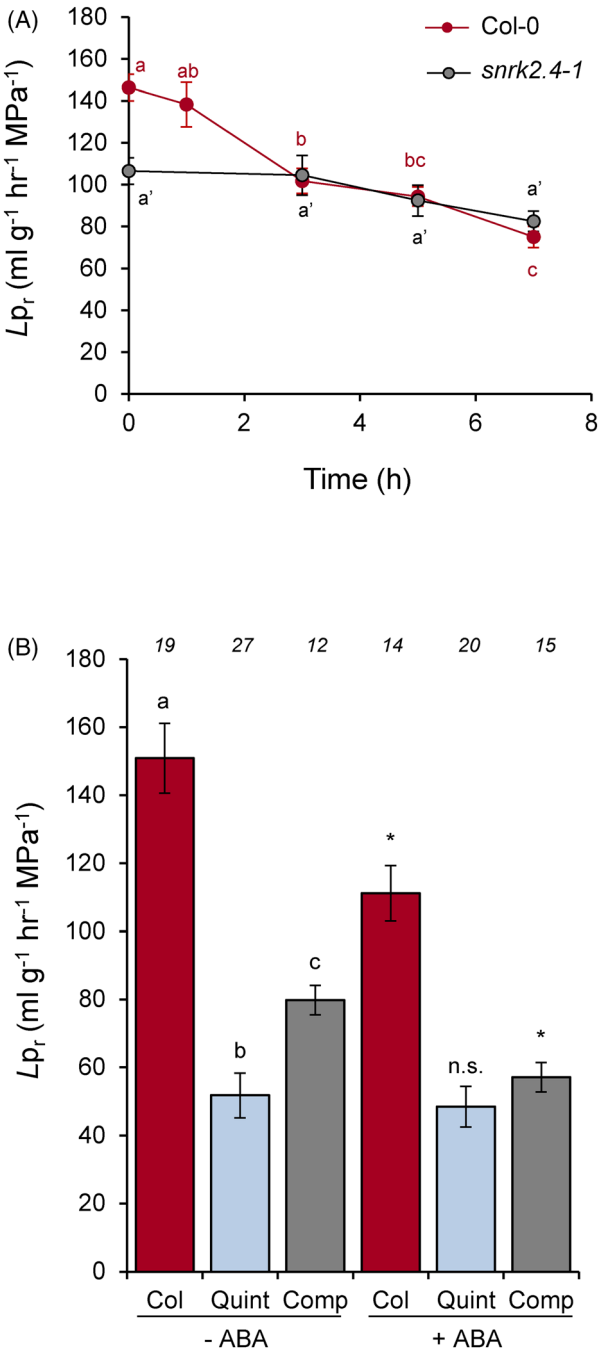

Figure 6. Effects of exogenous ABA on Lp_r of various *snrk2.4* and *pip* genotypes.
(A) Time-dependent effects of exogenous ABA application (1 μM at t = 0) on Lp_r of Col-0 and *snrk2.4-1* plants. Cumulated data (mean ± SE) from 6 independent experiments with n = 12–40 plants. Different letters (ANOVA) indicate statistical differences between kinetic points for the same genotype (Col-0: red; *snrk2.4-1*: black).
(B) Effects of ABA (1 μM, 5 h) on Lp_r of Col-0, a quintuple *pip* mutant (Quint) and the same genotype complemented with a GFP-PIP2;1 fusion (Comp). Data (mean ± SE) from 4 independent experiments and the number of individual plants indicated on the top. The three genotypes showed distinct Lp_r values in the absence of ABA (ANOVA; see different letters). A genotype-by genotype t-test analysis indicated that ABA inhibits Lp_r in Col-0 and Comp (*) but not Quint (not significant: n.s.).

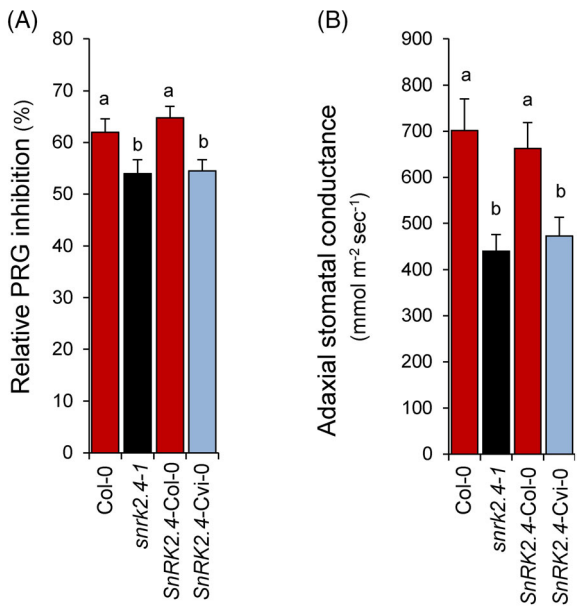

Figure 7. Growth and transpiration phenotypes of *snrk2.4* genotypes.
(A) Effects of 25 μM ABA on primary root growth (PRG) of Col-0, *snrk2.4-1*, and *snrk2.4-1* lines expressing Col-0 or Cvi-0 SnRK2.4 alleles. Relative inhibition (± SE) was determined with respect to primary root length of the same genotype on control plates lacking ABA. $n = 32$ plants.
(B) Mean adaxial stomatal conductance (± SE; $n = 20$) of Col-0, *snrk2.4-1*, and *snrk2.4-1* lines expressing Col-0 or Cvi-0 SnRK2.4 alleles.

phenotype could be complemented by expressing the Col-0 but not the Cvi-0 SnRK2.4 allele (Figure 7A; Figure S11f).

When inspecting intact leaves, we found that, under our growth conditions, *snrk2.4* mutants exhibited >30% reduction in stomatal conductance as compared to Col-0 (Figure 7B; Figure S11g). This defect could be compensated by the expression of the Col-0 SnRK2.4 but not the Cvi-0 SnRK2.4 allele. The same pattern of stomatal conductance was observed in both adaxial and abaxial sides of the leaves (Figure 7B; Figure S11g).

DISCUSSION

In the present work, we developed a quantitative genetics approach in a biparental (Cvi-0 x Col-0) segregating population to search for regulators of root hydraulics. In spite of recent advances in the field (Shahzad et al., 2016; Tang et al., 2018), this approach remains challenging due to the technical difficulty of phenotyping Lp_r at high throughput and to the strong dependence of this trait on the environmental conditions. Cloning of one of the major QTLs revealed that the SnRK2.4 protein kinase, which occurs in the two parents as two allelic forms with dramatically different functionalities, functions as an activator of aquaporins and contributes to up to 30% of constitutive Lp_r in Col-0.

Under resting conditions, aquaporins control 50–80% of Arabidopsis Lp_r depending upon natural accessions (Sutka et al., 2011), with for instance 5 PIP isoforms being responsible for 65% of Lp_r in Col-0 (Figure 6). Here, we found that *SnRK2.4* contributes to >30% of overall Lp_r of Col-0, acting on its azide-dependent component. This identifies this protein kinase as a potent regulator of root azide-sensitive aquaporins. Phosphorylation of PIPs is one of the key post-translational modifications that correlates well with Arabidopsis Lp_r and rosette hydraulic conductivity under numerous physiological stresses (Di Pietro et al., 2013; Prado et al., 2019). In addition, transgenic complementation has shown that multiple phosphorylation sites in the C-terminal domain of PIP2;1 govern its water transport activity in Arabidopsis leaves (Prado et al., 2013, 2019; Qing et al., 2016). In stomata, ABA- and flagellin-induced closure critically depends on phosphorylation of PIP2;1 at Ser121 (Grondin et al., 2015; Rodrigues et al., 2017), *SnRK2.6* being the most likely candidate for mediating these effects. The capacity of *SnRK2.4* to directly regulate aquaporins in roots was addressed along the same lines, taking PIP2;1 as a prototypic PIP isoform. BiFC assay revealed that Col-0 SnRK2.4 can directly interact with PIP2;1. The protein kinase also phosphorylated PIP2;1-derived peptides at Ser121 *in vitro*, and stimulated its water and H_2O_2 transport activity upon coexpression in oocytes and yeast cells. Mutational study in yeast suggested that protein kinase activity of Col-0 SnRK2.4 is required for its enhancing effects on PIP2;1. This is in agreement with the activating role of loop *B* (Ser121 in PIP2;1) phosphorylation, as pointed out by molecular dynamics studies (Törnroth-Horsefield et al., 2006) and H_2O_2 transport assays in transgenic wheat (Lu et al., 2022). Contrastingly, Cvi-0 SnRK2.4 failed in the *in vitro* phosphorylation, BiFC, and yeast growth assays, probably because it lacks part of a C-terminal regulatory domain and it is poorly expressed or instable in oocytes. More precisely, the Cvi-0 SnRK2.4 variant lacks the osmotic regulatory domain DI (amino acid residues 283–302) that stabilizes the catalytically essential αC helix of protein kinases, by aligning with αC within a hydrophobic pocket, in the amino terminal lobe of the protein (Yunta et al., 2011). Deletion of this domain abrogated the protein kinase activity of SnRK2.6/OST1 (Belin et al., 2006). Overall, results from the two heterologous expression systems, *Xenopus* oocytes, and yeast cells, are consistent with *in planta* data showing that, in contrast to Col-0 SnRK2.4, Cvi-0 SnRK2.4 cannot complement the constitutive Lp_r defects of *snrk2.4*. We propose that deletion of the DI domain in Cvi-0 SnRK2.4 represents a major causal polymorphism, although others may exist since *SnRK2.4* shows a 2-fold lower expression in Cvi-0 than Col-0 (Kawakatsu et al., 2016).

Despite the emerging functional importance of PIP phosphorylation at loop *B* (Grondin et al., 2015; Lu et al., 2022; Rodrigues et al., 2017; Törnroth-Horsefield

et al., 2006; Yaneff et al., 2016), all previous phosphoproteomic studies except a recent one in wheat (Lu et al., 2022) have failed to detect this phosphorylation *in planta* (Di Pietro et al., 2013; Van Wilder et al., 2008; Whiteman et al., 2008). Unfortunately, and at variance with the study by Lu et al. (2022), neither phosphoproteomics nor Phos-tag detection allowed us to detect loop *B* phosphorylation and thereby compare its abundance in Col-0 and *snrk2.4*. Yet, combination of our findings *in vitro* (Figure 3), in heterologous systems (Figures 4 and 5), and *in planta* (Figures 2C–E) clearly highlights the important role of Col-0 *SnRK2.4* to increase Lp_r under resting conditions. Therefore, we propose that the protein kinase mediates phosphorylation of PIPs at the well-conserved loop *B* phosphorylation site.

SnRK2.4 is a well-described member of the SnRK2 family. These protein kinases have long been identified as central players in plant hormonal and environmental stress signaling (Kulik et al., 2011). In complement to biochemical evidence for ABA-dependent activation, double and triple knock-out mutants for group II and III members have established their positive role in osmotic and ABA signaling (Fujii & Zhu, 2009; Fujita et al., 2009; Mizoguchi et al., 2010; Nakashima et al., 2009). At variance, group I members such as SnRK2.4 and SnRK2.10 are thought to be essentially involved in plant responses to osmotic and oxidative stresses (Kulik et al., 2012; McLoughlin et al., 2012). Here, we show that SnRK2.4 plays a genuine role in plants under resting conditions and exerts a key control of root hydraulics.

Recent studies in yeast (Ruschhaupt et al., 2019) indicate that similar to SnRK2.6, SnRK2.4 and its group I homologs have all hallmark to be part of core ABA signaling modules. Canonical group II and III SnRK2s show negative regulation by clade A PP2Cs that act as ABA co-receptors (Umezawa et al., 2009; Vlad et al., 2009). One of these, ABI1, was shown to also interact with SnRK2.4, to dephosphorylate Ser158, thereby inhibiting its activity (Kawakatsu et al., 2016). Functional analysis in yeast further revealed the inhibitory action of various clade A PP2Cs on group I SnRK2s including SnRK2.4 (Ruschhaupt et al., 2019). Whereas the readout was transcriptional stimulation of reporter expression, we analyzed in this study PIP2;1 stimulation by SnRK2.4 and inhibition of the response by PP2Cs. We found that PP2C expression without SnRK2.4 coexpression did not alter H_2O_2 transport by PIP2;1, consistent with a direct regulatory role of PP2Cs on SnRK2.4 activity (Krzywinska et al., 2016).

These observations prompted us to investigate a possible contribution of SnRK2.4 to ABA-dependent regulation of Lp_r. In guard cells, SnRK2s including SnRK2.6 are thought to mediate an ABA-dependent activation of PIP2;1 by ligand-receptor-mediated sequestering of the inhibitory PP2Cs (Grondin et al., 2015; Rodrigues et al., 2017). In contrast to stomata, Arabidopsis roots showed an inhibition of water permeability in response to high ABA concentration (1 μM) (Figure 6). Thus, in the presence of the hormone, ABA-dependent SnRK2s present in roots would act on molecular components that negatively target root aquaporins including PIP2;1. These would in turn dominate the direct positive effects of SnRK2.4 on their activity, which was revealed under resting conditions. ABA-induced induction of PP2Cs such as the Highly ABA-Induced (HAI) members, that act as effective inhibitors of ABA signaling (Tischer et al., 2017), might provide such down-regulatory mechanism. In such a scheme, the insensitivity of *snrk2.4* Lp_r to short term (<3 h) inhibition by exogenous ABA may be explained by a signaling defect. Alternatively, SnRK2.4 and ABA may independently target the same pool of root aquaporins, and the insensitivity of *snrk2.4* Lp_r to ABA may be due to a simple lack of activated aquaporins. Nevertheless, in the long term (>3 h), ABA seems to target aquaporins (including PIP2;1) in a SnRK2.4-independent manner.

The Lp_r phenotype of *snrk2.4* plants at resting conditions also challenges the classical view that SnRK2.4 is specifically activated in response to osmotic and salt stresses (Boudsocq et al., 2004). In plants under resting conditions, SnRK2.4 indeed shows a residual activation by as yet unknown factors, potentially the low endogenous levels of ABA. In support of this, yeast expression showed SnRK2.4 to be very ABA-sensitively regulated by the receptor complex RCAR11 and ABI1, compared to SnRK2.6 that was approximately a hundred times less sensitive (Ruschhaupt et al., 2019). The recent finding that Raf-like kinases act upstream of SnRK2s (Katsuta et al., 2020; Lin et al., 2020; Soma et al., 2020; Takahashi et al., 2020) as integrators of osmotic stress and ABA responses in plants opens interesting avenues to address the modes and amplitude of SnRK2.4 activation in plants under resting or stressing conditions.

While initially focused on root hydraulics, our work revealed that SnRK2.4 plays a more general role in regulating and integrating water transport throughout the whole plant. In addition to defects in ABA-dependent primary root growth inhibition, *snrk2.4* plants showed under resting conditions and with respect to Col-0, a significantly reduced stomatal conductance. This defect could be due to both a general hydraulic limitation and a genuine dysfunction of stomata.

In conclusion, the present work identifies *SnRK2.4* as a key component of root functions and plant water transport that exists in alternative forms in Arabidopsis. Adding to the proposed role of SnRK2.6 in ABA-dependent regulation of guard cell aquaporins (Grondin et al., 2015, Rodrigues et al., 2017), this work raises important questions about the functional overlap and specificity of SnRK2.4 with respect to other ABA-dependent or independent SnRK2s.

EXPERIMENTAL PROCEDURES

Plant materials and growth conditions

The *Arabidopsis thaliana* accessions Col-0 (186AV) and Cvi-0 (166AV), the core population of RILs (8RV) corresponding to an F8 generation obtained by crossing these accessions, and the fixed HIFs (8HV046 and 8HV062, named HIF046 and HIF062, respectively, in the main text) were obtained from the Versailles Arabidopsis Stock Center (Institut Jean-Pierre Bourgin, INRA, Versailles, France). For further details, see http://publiclines.versailles.inra.fr/. The T-DNA mutant lines *snrk2.4-1* [N653316 (SALK_080588C)] and *snrk2.4-2* [N653535 (SALK_146522C)] were obtained from the Nottingham Arabidopsis Stock Centre (NASC). The insertion of T-DNA in these lines was confirmed using a T-DNA left border (LBb1.3) primer and corresponding right (RP) primer. Homozygous mutant plants were characterized using an adequate pair of left (LP) and right (RP) primers (Table S2). For complementation of the quintuple *pip2;1-2 pip2;2-3 pip2;4-1 pip2;6-3 pip2;7-1* mutant (Quint), we used a proPIP2;1::GFP-PIP2;1 construct inserted in a pGWB501 vector. The construct was first introduced into a triple *pip2;1-2 pip2;2-3 pip2;4-1* mutant using the floral dipping method. The complemented line was obtained by crossing Quint itself with the triple *pip2;1-2 pip2;2-3 pip2;4-1* mutant expressing the proPIP2;1::GFP-PIP2;1 transgene.

Seeds were surface sterilized in 90% ethanol with 0.35% sodium hypochlorite for 7 min, and rinsed with 96% ethanol thrice. Surface sterilized seeds were sown on 0.5 × MS agar vertical plates [2.2 g L^{-1} MS (Sigma, Saint Quentin Fallavier, France), 1% sucrose (Euromedex, Souffel Weyersheim, France), 0.05% MES (Euromedex), and 0.7% agar (Sigma), pH 5.7 adjusted using KOH], and incubated for at least 2 days at 4°C in the dark for stratification. Seedlings were grown on these plates for 10 days in a growth chamber at 70% relative humidity (RH) and 20°C, with cycles of 16 h of light (250 μE m^{-2} sec^{-1}). They were transferred to a hydroponic medium as described previously (Javot et al., 2003). The plants were further grown for 12–13 days under the same growth conditions and phenotyped for Lp_r.

Root hydraulic measurements

Lp_r measurements were made on root systems of 22- to 23-day-old plants grown in hydroponic medium, treated or not with ABA. In brief, Arabidopsis detopped root systems were sealed at hypocotyl using a combination of plastic and metallic seals with a low-viscosity dental paste (President Light, Coltene, Switzerland) and inserted into a pressure chamber containing 50 ml hydroponic medium with or without ABA in a falcon tube. Lp_r data were obtained as described previously (Shahzad et al., 2016). Pressure chamber measurements were performed throughout the day, indistinctly of the treatment. We also checked that Lp_r values were independent of the time of day and, therefore, combined individual measurements according to treatments. For aquaporin inhibition experiments, excised roots were incubated in the presence of 1 mM NaN_3 and Lp_r was derived from continuous measurement of water flow (J_v) at 320 kPa until a new steady state J_v value was reached after 30 min.

QTL and fine mapping

Phenotypic data for root hydraulics [conductivity (Lp_r) and conductance (L_0)], plant growth [shoot dry weight (DWs), DWr, DWs/DWr], and bolting time were obtained from a core population of Cvi-0 × Col-0 RILs grown in hydroponic conditions. For each trait, 7–8 plants per RIL were phenotyped from four independent experiments. Multiple QTL mapping (MQM) was performed using R/qtl (Arends et al., 2010) as described previously (Shahzad et al., 2016).

Fixed HIFs were generated as described (Tuinstra et al., 1997) from segregating F7 RIL 8RV046 and 8RV062 and used for confirmation of Lprt18 and Lprb58, respectively. A heterozygous 8HV046 individual in the Lprt18 region was self-fertilized to develop a fine-mapping population, and a total of 152 individuals recombined within the candidate interval were identified. These recombinant HIFs (rHIFs) were further genotyped with additional markers between c1_02212 and msat1.10 markers in order to locate the recombination breakpoint (primer sequences of markers are provided in Table S2) (Figure 2A). Twelve rHIFs were phenotypically tested in a 'progeny testing' process to discern if genotypic segregation was linked with segregation of Lp_r phenotype (Loudet et al., 2008).

Quantitative and molecular complementation

For quantitative complementation, advanced rHIFs (arHIFs) were developed as described (Loudet et al., 2008) by crossing two closely related rHIFs (rHIF046-64 and rHIF046-99) differing for a small interval of 50 kb within Lprt18. Plants carrying one of the two allelic forms, arHIF046-Cvi-0 or arHIF046-Col-0, were used for making independent reciprocal crosses with *snrk2.4-1* and Col-0 plants. F1 plants originating from these crosses were phenotyped for Lp_r, and each individual plant was genotyped using the IND1.03647 marker to ensure that it was a real F1 with the expected allelic combinations. For molecular complementation, a 3752 bp genomic region (Chr1: 3655576–3 659 328, corresponding to Col-0 TAIR10 sequence) harboring *SnRK2.4* was PCR-amplified from Cvi-0 or Col-0 using iProof™ High-Fidelity PCR Kit (Bio-Rad, Marnes-La-Coquette, France). Primer sequences are provided in Table S2. The *SnRK2.4* amplicons were cloned in a plant expression vector (pGreen 0179) and introduced into *snrk2.4-1* plants using the floral dip method (Clough & Bent, 1998). For each construct, three independent homozygous transgenic lines were selected in T2 generation on hygromycin B (30 mg L^{-1}) and were phenotyped for Lp_r.

Quantitative real-time (qRT)-PCR

Total RNA was isolated using an SV Total RNA Isolation System (Promega, Charbonnières-Les-Bains, France) from roots of Col-0 and *snrk2.4* plants grown in hydroponics. Two μg of total RNA were used for first strand cDNA synthesis using M-MLV Reverse Transcriptase, RNase H Minus, Point Mutant (Promega), and Oligo $(dT)_{15}$ Primer (Promega) in a final volume of 25 μl, according to the manufacturer's instructions. qRT-PCRs were performed in 384-well plates with a LightCycler 480 Real-Time PCR System (Roche Diagnostics, Meylan, France) using 0.1 μl first strand cDNA as template. cDNA amplification was monitored using SYBR Green at an annealing temperature of 57°C as described previously (Shahzad et al., 2010). Transcript abundance was expressed relative to *EF1α* (At1g07920) transcripts in a Col-0 sample used as calibrator and, in all samples, relative to the average of *UBC21* (At5g25760) and *EF1α* transcripts used as reference genes. The primer sequences used are described in Table S2.

ELISA assays

For experiments aimed at quantifying the overall abundance of PIP1 and PIP2 aquaporins, plants of Col-0 and *snrk2.4* were cultured in hydroponics under standard conditions. Total proteins from the roots were purified as previously described (Boursiac et al., 2005). The ELISA assays were performed as described

(Santoni et al., 2003). 0.5 μg of protein extracts were loaded in triplicate in a carbonate buffer (30 mM Na_2CO_3, 60 mM $NaHCO_3$, at pH9.5) on ELISA plates (Nunc Maxisorp®, eBioscience SAS, France). The anti-PIP1 and anti-PIP2 antibodies used for the detection of PIPs were as described (Li et al., 2015).

Bimolecular fluorescence complementation and water permeability (P_f) measurements in *Xenopus* oocytes

The PIP2;1 coding sequence was cloned in fusion with YFP^C and YFP^N in a 35S-SPYCE and 35S-SPYNE vector, respectively (Waadt et al., 2008). The constructs were then PCR amplified and cloned into a modified pGEMHE *Xenopus laevis* oocyte expression vector (Fisher Scientific, Illkirch Graffenstaden, France). A corresponding YFP^N-SnRK2.4 construct was obtained by substituting an *Apa*1-*Eco*R1 fragment in the former plasmid with the SnRK2.4 coding sequence. cRNA production, expression in oocytes, and P_f measurements were performed as described (Maurel et al., 1993) and fluorescence quantification was performed as explained in the previous sections. To determine the expression level of the BiFC constructs, oocytes extracts were analyzed by Western blot using an anti-YFPn antibody (abm, Vancouver, Canada). In brief, oocytes were ground in a RIPA buffer (abm), incubated for 25 min on ice, and centrifuged for 15 min at 7500 *g*. The supernatant was centrifuged again for 2 min at 10000 *g* and 9 μl of the resulting supernatant was mixed with 3 μl of Laemmli 4X prior to SDS-PAGE and immunoblotting.

Sub-cellular localization of PIP2;1

An RFP-PIP2;1 fusion protein under the control of a 35S promoter was obtained by cloning in a pB7WGR2 plant expression vector (Bellati et al., 2016) and introduced into Col-0 and *snrk2.4-1* genotypes using the floral dip method (Clough & Bent, 1998). For both Col-0 and *snrk2.4-1* genotypes, five independent transgenic lines were characterized. Plants expressing RFP protein fusions were observed using a Leica SP8 confocal laser-scanning microscope with a 40 × NA.1.1 objective and a 561 nm laser. Light was collected between 580 and 620 nm. In the case of oocytes expressing constructs fused to YFP^C or YFP^N, a 20×/0.3 Dry objective and the 488 nm line of the argon were used. Fluorescence emission was collected between 520 and 560 nm. For quantitative measurement of PIP2;1 abundance (in plants) and split YFP experiments (in oocytes), the laser power, pinhole and gain settings of the confocal microscope were identical among different treatments. Calculation of mean pixel intensity was obtained for a set of defined regions of interest (ROI) after background subtraction (ImageJ).

Protein purification and kinase assays

The SnRK2.4 coding DNA sequence was amplified by PCR from cDNA of Col-0 and Cvi-0 using PfU DNA polymerase (Promega), and cloned into a pGEX-6P-1 expression vector (Fisher Scientific). Primer sequences are listed in Table S2. The recombinant vector was transformed in BL21 Rosetta bacteria for protein expression. Production was induced with 0.1 mM IPTG for 3 h at 28°C. Recombinant glutathione-S-transferase(GST)::SnRK2.4 fusion proteins were purified as described previously (Shahzad et al., 2016). Amicon Ultra-15 30 K filtration unit (Millipore, Molsheim, France) was used to concentrate proteins which were stored at −50°C in 30% glycerol. The concentration of proteins were determined by a Bradford protein assay (Bradford, 1976).

Kinase activity was determined in a solution containing 50 mM KCl, 10 mM $MgCl_2$, 5 mM $MnCl_2$, 25 mM glycerophosphate, 1 mM DTT, 50 mM HEPES pH 7.5, 500 ng SnRK2.4 protein, 200 μM of the indicated PIP2;1 peptides, 100 μM ^{32}ATP (200 Ci mol^{-1}). Peptide sequences were as follows: Loop B; MACTAGISGGHINPAVTFGLFLARKVSLPRAKKK, and Cter; MASKSLGSFRSAANVKKK. Kinase assays were carried out as described (Shahzad et al., 2016).

Yeast expression and growth assays

The expression constructs for SnRK2.4 and PP2Cs for yeast and yeast transformation were reported earlier (Ruschhaupt et al., 2019). The cloning of the SnRK2.4 alleles and PIP2;1 of Arabidopsis was performed accordingly. Briefly, cDNAs were cloned into level I (LI_Bpil) vector of the Golden Gate Cloning system (Chiasson et al., 2019). All LI vectors were verified for correctness by DNA sequence analysis. PIP expression constructs were assembled in the level II vector (LII) pYEAST_LII_2-3_CEN_HIS with ADH1 promoter and TDH1 terminator (tTDH1) for PIP2;1, pYEAST_LII_3-4_CEN_TRP with TDH3 promoter (pTDH3) and tTDH1 for SnRK2.4 variants, and pYEAST_LII_1-2_CEN_LEU with pTDH3 and tTDH1 for expression of PP2Cs. Yeast transformation of strain BMA64-1A (EUROSCARF, Uni-Frankfurt, Germany) and colony selection were performed according to Amberg et al. (2005). Freshly transformed yeast colonies were inoculated in 0.5 ml supplemented synthetic dextrose (SD) medium containing 2% glucose and incubated at 30°C in a Thermoshake-THO500 gyratory shaker (Gerhardt, Königswinter, Germany) at 200 rpm for 16–18 h. After overnight growth, 4.5 mL SD medium was added and the culture was allowed to reach OD_{600} between 0.6 and 0.8. Cells were sedimented (1500 *g*, 5 min) and the cell density was adjusted to OD_{600} of 0.1. Ten μl of the cell suspension were spotted as a 10-fold dilution series on freshly prepared SD agar plates containing either no or 0.2 mM H_2O_2 and incubated at 30° C for 2 days.

Stopped-flow spectrophotometry on isolated spheroplasts

Cells were grown in 25 ml of YPD medium [0.5% (w/v) yeast extract, 1% (w/v) peptone, 2% (w/v) glucose], with orbital shaking, at 28°C and harvested in the exponential phase (OD600 ≈ 1) by centrifugation (18 000 *g*) for 5 min at 4°C, and washed once with H_2O and once with 1,2 M sorbitol. Cells are resuspended in 2.5 ml of digestion buffer (1.2 M Sorbitol, 100 mM Sodium Phosphate (pH 6,5)) containing 20 mM DTT and 500 U of Lyticase and incubated at 30°C. When the digestion was complete, the spheroplasts were centrifuged for 4 min at 1300 *g* (4°C), and carefully washed twice in 5 ml of digestion buffer (-DTT). The pellet was finally carefully resuspended in 2 ml of digestion buffer (-DTT) and stored in ice for 10 min (4°C) before stopped-flow experiments. The spheroplast preparations were homogeneous, spheroplasts were spherical in shape, and their average size was determined under light microscopy. Kinetics of spheroplast volume adjustment were followed by 90° light scattering at λ_{ex} = 515 nm. Measurements were performed at 15°C, in a SFM3 stopped-flow spectrophotometer (Biologic, Claix, France) essentially as previously described (Maurel et al., 1997). Briefly, spheroplasts were diluted 10-fold into the digestion buffer. They were then loaded in the stopped-flow device and mixed (dead time <3 ms) with an equal volume of the digestion buffer but with a concentration of 1.8 M sorbitol. The traces from more than 10 individual stopped-flow acquisitions were averaged and the curves were fitted to single exponential equations to determine an exponential rate constant k_{exp}. The osmotic water permeability coefficient (P_f) was computed from the light scattering time course and the size of membrane vesicles according to the following equation: $P_f = k_{exp} \cdot V_o / A \cdot V_w \cdot C_{out}$ where V_o is the initial mean spheroplast volume, A is the mean spheroplast surface, V_w is the molar volume of water, and C_{out} is the external osmolality.

Root growth assays

Seedlings were germinated on a ½ MS medium, transferred after 3 days onto the same medium in the absence or presence of 25 μM ABA, and further grown vertically for 7 days. Primary root length (PRL) was measured using ImageJ.

Stomatal assays

Stomatal conductance was measured using an AP4 leaf porometer on the abaxial and adaxial sides of rosette leaves of 22-day-old plants cultured in hydroponics.

Statistical analyses

Unless otherwise stated, the statistical significance of data at $P < 0.05$ was assessed using either Student's *t*-test (see *) or one-way ANOVA (see letters). The number of biological replicates (*n*) is indicated in figures or figure legends.

ACKNOWLEDGMENTS

This work was supported by grants of the Agence Nationale de la Recherche (ANR-11-BSV6-018; ANR-18-CE92-0055-01) and a research contract from Syngenta (HydroRoot). EG was supported by the Deutsche Forschung Gemeinschaft. We thank Dr Anton R. Schäffner for providing the triple and quintuple *pip* mutant, Dr Jörg Kudla for the gift of BiFC constructs, Jérémy Dehors for initial oocyte expression experiments, and Xavier Dumont for the production of transgenic *proPIP2;1::GFP-PIP2;1* plants. We also thank Montpellier Ressources Imagerie (MRI) and the PHIV platform for access and technical support in microscopy. The IJPB benefits from the support of Saclay Plant Sciences-SPS integrated into France 2030 (reference no. ANR-11-IDEX-0003-02). This work received the support of IJPB's Plant Observatory technological platforms.

AUTHOR CONTRIBUTIONS

The experiments were conceived and designed by ZS, OL, EG, and CM with input from VS, and mainly carried out by ZS. CT-R carried out protein kinase production and assays, qPCR analyses, and functional studies in oocytes. MC generated genetic materials for fine mapping. MA characterized the effects of exogenous ABA. JR and LV performed yeast expression experiments. AM contributed to confocal microscopy. AA provided materials and resources for PIP2 phosphorylation studies. ZS, OL, CT-R, JR, LV, AM, and CM analyzed the data. ZS and CM wrote the paper.

SUPPORTING INFORMATION

Additional Supporting Information may be found in the online version of this article.

Table S1. Means, ranges, and broad-sense heritabilities (h^2) of hydraulic, growth, and developmental phenotypic traits in two parental lines (Cvi-0 and Col-0) and in RILs derived from their cross.

Table S2. List of primer sequences used in the study.

Figure S1. Frequency distribution of root hydraulics (Lp_r, L_0), root and shoot growth (DW_r, DW_s, DW_s/DW_r), and bolting time traits in a Cvi-0 × Col-0 RIL population.

Figure S2. Lp_r (mean ± SE) of HIF062-Cvi-0 and HIF062-Col-0 lines.

Figure S3. Protein sequence alignment of SnRK2.4 allelic forms from Col-0, Cvi-0, and corresponding genotypes of HIF046.

Figure S4. Molecular complementation of *snrk2.4-1* with Col-0 and Cvi-0 *SnRK2.4* genomic regions.

Figure S5. Expression of PIP in Col-0 and *snrk2.4* plants.

Figure S6. Expression of recombinant GST-SnRK2.4 fusions in *E. coli*.

Figure S7. Expression analysis of SnRK2.4 in yeast.

Figure S8. ABA-response-regulatory PP2Cs counteract SnRK2.4-mediated stimulation of PIP2;1.

Figure S9. Lp_r of HIF046-Cvi-0 and HIF046-Col-0 lines in the absence of (Mock) or after treatment with ABA (1 μM) or NaCl (150 mM) for 3 h.

Figure S10. Lp_r of Col-0, *snrk2.4-1*, and *snrk2.4-1* lines expressing Col-0 or Cvi-0 *SnRK2.4* alleles in the absence of or after treatment with 1 μM ABA for 3 h.

Figure S11. Expression and function of SnRK2.4 in roots and shoots.

REFERENCES

Amberg, D.C., **Burke, D.J.** & **Strathern, J.N.** (2005) *Methods in yeast genetics: a Cold Spring Harbor Laboratory course manual*. Cold Spring Harbor, NY: Cold Spring Harbor Laboratory Press.

Arends, D., **Prins, P.**, **Jansen, R.C.** & **Broman, K.W.** (2010) R/QTL: high-throughput multiple QTL mapping. *Bioinformatics*, **26**, 2990–2992.

Belin, C., **de Franco, P.O.**, **Bourbousse, C.**, **Chaignepain, S.**, **Schmitter, J.M.**, **Vavasseur, A.** ***et al.*** (2006) Identification of features regulating OST1 kinase activity and OST1 function in guard cells. *Plant Physiology*, **141**, 1316–1327.

Bellati, J., **Champeyroux, C.**, **Hem, S.**, **Rofidal, V.**, **Krouk, G.**, **Maurel, C.** ***et al.*** (2016) Novel aquaporin regulatory mechanisms revealed by interactomics. *Molecular & Cellular Proteomics*, **15**, 3473–3487.

Boudsocq, M., **Barbier-Brygoo, H.** & **Lauriere, C.** (2004) Identification of nine sucrose nonfermenting 1-related protein kinases 2 activated by hyperosmotic and saline stresses in *Arabidopsis thaliana*. *The Journal of Biological Chemistry*, **279**, 41758–41766.

Boursiac, Y., **Chen, S.**, **Luu, D.-T.**, **Sorieul, M.**, **van den Dries, N.** & **Maurel, C.** (2005) Early effects of salinity on water transport in *Arabidopsis* roots. Molecular and cellular features of aquaporin expression. *Plant Physiology*, **139**, 790–805.

Boursiac, Y., **Protto, V.**, **Rishmawi, L.** & **Maurel, C.** (2022) Experimental and conceptual approaches to root water transport. *Plant and Soil*, **478**, 349–370.

Bradford, M.M. (1976) A rapid and sensitive method for the quantitation of microgram quantities of protein utilizing the principle of protein-dye binding. *Analytical Biochemistry*, **72**, 248–254.

Brandt, B., **Brodsky, D.E.**, **Xue, S.**, **Negi, J.**, **Iba, K.**, **Kangasjarvi, J.** ***et al.*** (2012) Reconstitution of abscisic acid activation of SLAC1 anion channel by CPK6 and OST1 kinases and branched ABI1 PP2C phosphatase action. *Proceedings of the National Academy of Sciences of the United States of America*, **109**, 10593–10598.

Chaumont, F. & **Tyerman, S.D.** (2014) Aquaporins: highly regulated channels controlling plant water relations. *Plant Physiology*, **164**, 1600–1618.

Chiasson, D., **Gimenez-Oya, V.**, **Bircheneder, M.**, **Bachmaier, S.**, **Studtrucker, T.**, **Ryan, J.** ***et al.*** (2019) A unified multi-kingdom Golden Gate cloning platform. *Scientific Reports*, **9**, 10131.

Clough, S.J. & **Bent, A.F.** (1998) Floral dip: a simplified method for *Agrobacterium*-mediated transformation of *Arabidopsis thaliana*. *The Plant Journal*, **16**, 735–743.

Cutler, S.R., **Rodriguez, P.L.**, **Finkelstein, R.R.** & **Abrams, S.R.** (2010) Abscisic acid: emergence of a core signaling network. *Annual Review of Plant Biology*, **61**, 651–679.

Di Pietro, M., **Vialaret, J.**, **Li, G.**, **Hem, S.**, **Rossignol, M.**, **Maurel, C.** ***et al.*** (2013) Coordinated post-translational responses of aquaporins to abiotic and nutritional stimuli in *Arabidopsis* roots. *Molecular & Cellular Proteomics*, **12**, 3886–3897.

Fan, W., **Li, J.**, **Jia, J.**, **Wang, F.**, **Cao, C.**, **Hu, J.** ***et al.*** (2015) Pyrabactin regulates root hydraulic properties in maize seedlings by affecting PIP

aquaporins in a phosphorylation-dependent manner. *Plant Physiology and Biochemistry*, **94**, 28–34.

Fujii, H., Chinnusamy, V., Rodrigues, A., Rubio, S., Antoni, R., Park, S.Y. *et al.* (2009) In vitro reconstitution of an abscisic acid signalling pathway. *Nature*, **462**, 660–664.

Fujii, H. & Zhu, J.K. (2009) Arabidopsis mutant deficient in 3 abscisic acid-activated protein kinases reveals critical roles in growth, reproduction, and stress. *Proceedings of the National Academy of Sciences of the United States of America*, **106**, 8380–8385.

Fujita, Y., Nakashima, K., Yoshida, T., Katagiri, T., Kidokoro, S., Kanamori, N. *et al.* (2009) Three SnRK2 protein kinases are the main positive regulators of abscisic acid signaling in response to water stress in Arabidopsis. *Plant & Cell Physiology*, **50**, 2123–2132.

Grondin, A., Rodrigues, O., Verdoucq, L., Merlot, S., Leonhardt, N. & Maurel, C. (2015) Aquaporins contribute to ABA-triggered stomatal closure through OST1-mediated phosphorylation. *Plant Cell*, **27**, 1945–1954.

Hose, E., Steudle, E. & Hartung, W. (2000) Abscisic acid and hydraulic conductivity of maize roots: a study using cell- and root-pressure probes. *Planta*, **211**, 874–882.

Javot, H., Lauvergeat, V., Santoni, V., Martin-Laurent, F., Guclu, J., Vinh, J. *et al.* (2003) Role of a single aquaporin isoform in root water uptake. *Plant Cell*, **15**, 509–522.

Katsuta, S., Masuda, G., Bak, H., Shinozawa, A., Kamiyama, Y., Umezawa, T. *et al.* (2020) Arabidopsis Raf-like kinases act as positive regulators of subclass III SnRK2 in osmostress signaling. *The Plant Journal*, **103**, 634–644.

Kawa, D., Meyer, A.J., Dekker, H.L., Abd-El-Haliem, A.M., Gevaert, K., Van De Slijke, E. *et al.* (2020) SnRK2 protein kinases and mRNA Decapping machinery control root development and response to salt. *Plant Physiology*, **182**, 361–377.

Kawakatsu, T., Huang, S.C., Jupe, F., Sasaki, E., Schmitz, R.J., Urich, M.A. *et al.* (2016) Epigenomic diversity in a global collection of *Arabidopsis thaliana* accessions. *Cell*, **166**, 492–505.

Krzywinska, E., Bucholc, M., Kulik, A., Ciesielski, A., Lichocka, M., Debski, J. *et al.* (2016) Phosphatase ABI1 and okadaic acid-sensitive phosphoprotein phosphatases inhibit salt stress-activated SnRK2.4 kinase. *BMC Plant Biology*, **16**, 136.

Kulik, A., Anielska-Mazur, A., Bucholc, M., Koen, E., Szymanska, K., Zmienko, A. *et al.* (2012) SNF1-related protein kinases type 2 are involved in plant responses to cadmium stress. *Plant Physiology*, **160**, 868–883.

Kulik, A., Wawer, I., Krzywinska, E., Bucholc, M. & Dobrowolska, G. (2011) SnRK2 protein kinases—key regulators of plant response to abiotic stresses. *OMICS*, **15**, 859–872.

Li, G., Boudsocq, M., Hem, S., Vialaret, J., Rossignol, M., Maurel, C. *et al.* (2015) The calcium-dependent protein kinase CPK7 acts on root hydraulic conductivity. *Plant, Cell & Environment*, **38**, 1312–1320.

Li, X., Wang, X., Yang, Y., Li, R., He, Q., Fang, X. *et al.* (2011) Single-molecule analysis of PIP2;1 dynamics and partitioning reveals multiple modes of *Arabidopsis* plasma membrane aquaporin regulation. *Plant Cell*, **23**, 3780–3797.

Lin, Z., Li, Y., Zhang, Z., Liu, X., Hsu, C.C., Du, Y. *et al.* (2020) A RAF-SnRK2 kinase cascade mediates early osmotic stress signaling in higher plants. *Nature Communications*, **11**, 613.

Loudet, O., Michael, T.P., Burger, B.T., Le Metté, C., Mockler, T.C., Weigel, D. *et al.* (2008) A zinc knuckle protein that negatively controls morning-specific growth in *Arabidopsis thaliana*. *Proceedings of the National Academy of Sciences of the United States of America*, **105**, 17193–17198.

Lu, K., Chen, X., Yao, X., An, Y., Wang, X., Qin, L. *et al.* (2022) Phosphorylation of a wheat aquaporin at two sites enhances both plant growth and defense. *Molecular Plant*, **15**, 1772–1789.

Mahdieh, M. & Mostajeran, A. (2009) Abscisic acid regulates root hydraulic conductance via aquaporin expression modulation in *Nicotiana tabacum*. *Journal of Plant Physiology*, **166**, 1993–2003.

Maurel, C., Boursiac, Y., Luu, D.T., Santoni, V., Shahzad, Z. & Verdoucq, L. (2015) Aquaporins in plants. *Physiological Reviews*, **95**, 1321–1358.

Maurel, C. & Nacry, P. (2020) Root architecture and hydraulics converge for acclimation to changing water availability. *Nature Plants*, **6**, 744–749.

Maurel, C., Reizer, J., Schroeder, J.I. & Chrispeels, M.J. (1993) The vacuolar membrane protein g-TIP creates water specific channels in *Xenopus* oocytes. *The EMBO Journal*, **12**, 2241–2247.

Maurel, C., Tacnet, F., Guclu, J., Guern, J. & Ripoche, P. (1997) Purified vesicles of tobacco cell vacuolar and plasma membranes exhibit dramatically different water permeability and water channel activity. *Proceedings of the National Academy of Sciences of the United States of America*, **94**, 7103–7108.

McLoughlin, F., Galvan-Ampudia, C.S., Julkowska, M.M., Caarls, L., van der Does, D., Laurière, C. *et al.* (2012) The Snf1-related protein kinases SnRK2.4 and SnRK2.10 are involved in maintenance of root system architecture during salt stress. *The Plant Journal*, **72**, 436–449.

Mizoguchi, M., Umezawa, T., Nakashima, K., Kidokoro, S., Takasaki, H., Fujita, Y. *et al.* (2010) Two closely related subclass II SnRK2 protein kinases cooperatively regulate drought-inducible gene expression. *Plant & Cell Physiology*, **51**, 842–847.

Nakashima, K., Fujita, Y., Kanamori, N., Katagiri, T., Umezawa, T., Kidokoro, S. *et al.* (2009) Three Arabidopsis SnRK2 protein kinases, SRK2D/SnRK2.2, SRK2E/SnRK2.6/OST1 and SRK2I/SnRK2.3, involved in ABA signaling are essential for the control of seed development and dormancy. *Plant & Cell Physiology*, **50**, 1345–1363.

Olaetxea, M., Mora, V., Bacaicoa, E., Garnica, M., Fuentes, M., Casanova, E. *et al.* (2015) Abscisic acid regulation of root hydraulic conductivity and aquaporin gene expression is crucial to the plant shoot growth enhancement caused by rhizosphere humic acids. *Plant Physiology*, **169**, 2587–2596.

Prado, K., Boursiac, Y., Tournaire-Roux, C., Monneuse, J.-M., Postaire, O., Da Ines, O. *et al.* (2013) Regulation of *Arabidopsis* leaf hydraulics involves light-dependent phosphorylation of aquaporins in veins. *Plant Cell*, **25**, 1029–1039.

Prado, K., Cotelle, V., Li, G., Bellati, J., Tang, N., Tournaire-Roux, C. *et al.* (2019) Oscillating aquaporin phosphorylation and 14-3-3 proteins mediate the circadian regulation of leaf hydraulics. *Plant Cell*, **31**, 417–429.

Prak, S., Hem, S., Boudet, J., Viennois, G., Sommerer, N., Rossignol, M. *et al.* (2008) Multiple phosphorylations in the C-terminal tail of plant plasma membrane aquaporins. Role in sub-cellular trafficking of *At*PIP2;1 in response to salt stress. *Molecular & Cellular Proteomics*, **7**, 1019–1030.

Qing, D., Yang, Z., Li, M., Wong, W.S., Guo, G., Liu, S. *et al.* (2016) Quantitative and functional phosphoproteomic analysis reveals that ethylene regulates water transport via the C-terminal phosphorylation of aquaporin PIP2;1 in *Arabidopsis*. *Molecular Plant*, **9**, 158–174.

Raghavendra, A.S., Gonugunta, V.K., Christmann, A. & Grill, E. (2010) ABA perception and signalling. *Trends in Plant Science*, **15**, 395–401.

Rodrigues, O., Reshetnyak, G., Grondin, A., Saijo, Y., Leonhardt, N., Maurel, C. *et al.* (2017) Aquaporins facilitate hydrogen peroxide entry into guard cells to mediate ABA- and pathogen-triggered stomatal closure. *Proceedings of the National Academy of Sciences of the United States*, **114**, 9200–9205.

Ruschhaupt, M., Mergner, J., Mucha, S., Papacek, M., Doch, I., Tischer, S.V. *et al.* (2019) Rebuilding core abscisic acid signaling pathways of Arabidopsis in yeast. *The EMBO Journal*, **38**, e101859.

Santoni, V., Vinh, J., Pflieger, D., Sommerer, N. & Maurel, C. (2003) A proteomic study reveals novel insights into the diversity of aquaporin forms expressed in the plasma membrane of plant roots. *The Biochemical Journal*, **372**, 289–296.

Scharwies, J.D. & Dinneny, J.R. (2019) Water transport, perception, and response in plants. *Journal of Plant Research*, **132**, 311–324.

Shahzad, Z., Canut, M., Tournaire-Roux, C., Martinière, A., Boursiac, Y., Loudet, O. *et al.* (2016) A potassium-dependent oxygen sensing pathway regulates plant root hydraulics. *Cell*, **167**, 87–98.

Shahzad, Z., Gosti, F., Frerot, H., Lacombe, E., Roosens, N., Saumitou-Laprade, P. *et al.* (2010) The five AhMTP1 zinc transporters undergo different evolutionary fates towards adaptive evolution to zinc tolerance in *Arabidopsis halleri*. *PLoS Genetics*, **6**, e1000911.

Soma, F., Mogami, J., Yoshida, T., Abekura, M., Takahashi, F., Kidokoro, S. *et al.* (2017) ABA-unresponsive SnRK2 protein kinases regulate mRNA decay under osmotic stress in plants. *Nature Plants*, **3**, 16204.

Soma, F., Takahashi, F., Suzuki, T., Shinozaki, K. & Yamaguchi-Shinozaki, K. (2020) Plant Raf-like kinases regulate the mRNA population upstream of ABA-unresponsive SnRK2 kinases under drought stress. *Nature Communications*, **11**, 1373.

Sutka, M., Li, G., Boudet, J., Boursiac, Y., Doumas, P. & Maurel, C. (2011) Natural variation of root hydraulics in *Arabidopsis* grown in normal and salt stress conditions. *Plant Physiology*, **155**, 1264–1276.

Takahashi, Y., **Zhang, J.**, **Hsu, P.K.**, **Ceciliato, P.H.O.**, **Zhang, L.**, **Dubeaux, G.** ***et al.*** (2020) MAP3Kinase-dependent SnRK2-kinase activation is required for abscisic acid signal transduction and rapid osmotic stress response. *Nature Communications*, **11**, 12.

Tang, N., **Shahzad, Z.**, **Lonjon, F.**, **Loudet, O.**, **Vailleau, F.** & **Maurel, C.** (2018) Natural variation at *XND1* impacts root hydraulics and trade-off for stress responses in Arabidopsis. *Nature Communications*, **9**, 3884.

The 1001 Genomes Consortium. (2016) 1,135 genomes reveal the global pattern of polymorphism in *Arabidopsis thaliana*. *Cell*, **166**, 481–491.

Tischer, S.V., **Wunschel, C.**, **Papacek, M.**, **Kleigrewe, K.**, **Hofmann, T.**, **Christmann, A.** ***et al.*** (2017) Combinatorial interaction network of abscisic acid receptors and coreceptors from Arabidopsis thaliana. *Proceedings of the National Academy of Sciences of the United States of America*, **114**, 10280–10285.

Törnroth-Horsefield, S., **Wang, Y.**, **Hedfalk, K.**, **Johanson, U.**, **Karlsson, M.**, **Tajkhorshid, E.** ***et al.*** (2006) Structural mechanism of plant aquaporin gating. *Nature*, **439**, 688–694.

Tournaire-Roux, C., **Sutka, M.**, **Javot, H.**, **Gout, E.**, **Gerbeau, P.**, **Luu, D.T.** ***et al.*** (2003) Cytosolic pH regulates root water transport during anoxic stress through gating of aquaporins. *Nature*, **425**, 393–397.

Tuinstra, M.R., **Ejeta, G.** & **Goldsbrough, P.B.** (1997) Heterogeneous inbred family (HIF) analysis: a method for developing near-isogenic lines that differ at quantitative trait loci. *Theoretical and Applied Genetics*, **95**, 1005–1011.

Umezawa, T., **Sugiyama, N.**, **Mizoguchi, M.**, **Hayashi, S.**, **Myouga, F.**, **Yamaguchi-Shinozaki, K.** ***et al.*** (2009) Type 2C protein phosphatases directly regulate abscisic acid-activated protein kinases in Arabidopsis. *Proceedings of the National Academy of Sciences of the United States of America*, **106**, 17588–17593.

Van Wilder, V., **Miecielica, U.**, **Degand, H.**, **Derua, R.**, **Waelkens, E.** & **Chaumont, F.** (2008) Maize plasma membrane aquaporins belonging to the PIP1 and PIP2 subgroups are *in vivo* phosphorylated. *Plant & Cell Physiology*, **49**, 1364–1377.

Vlad, F., **Rubio, S.**, **Rodrigues, A.**, **Sirichandra, C.**, **Belin, C.**, **Robert, N.** ***et al.*** (2009) Protein phosphatases 2C regulate the activation of the Snf1-related kinase OST1 by abscisic acid in Arabidopsis. *Plant Cell*, **21**, 3170–3184.

Waadt, R., **Schmidt, L.K.**, **Lohse, M.**, **Hashimoto, K.**, **Bock, R.** & **Kudla, J.** (2008) Multicolor bimolecular fluorescence complementation reveals simultaneous formation of alternative CBL/CIPK complexes in planta. *The Plant Journal*, **56**, 505–516.

Weigel, D. (2012) Natural variation in Arabidopsis: from molecular genetics to ecological genomics. *Plant Physiology*, **158**, 2–22.

Whiteman, S.A., **Nuhse, T.S.**, **Ashford, D.A.**, **Sanders, D.** & **Maathuis, F.J.** (2008) A proteomic and phosphoproteomic analysis of *Oryza sativa* plasma membrane and vacuolar membrane. *The Plant Journal*, **56**, 146–156.

Wudick, M.M., **Li, X.**, **Valentini, V.**, **Geldner, N.**, **Chory, J.**, **Lin, J.** ***et al.*** (2015) Subcellular redistribution of root aquaporins induced by hydrogen peroxide. *Molecular Plant*, **8**, 1103–1114.

Yan, J., **Wang, P.**, **Wang, B.**, **Hsu, C.C.**, **Tang, K.**, **Zhang, H.** ***et al.*** (2017) The SnRK2 kinases modulate miRNA accumulation in Arabidopsis. *PLoS Genetics*, **13**, e1006753.

Yaneff, A., **Sigaut, L.**, **Gomez, N.**, **Aliaga Fandino, C.**, **Alleva, K.**, **Pietrasanta, L.I.** ***et al.*** (2016) Loop B serine of a plasma membrane aquaporin type PIP2 but not PIP1 plays a key role in pH sensing. *Biochimica et Biophysica Acta*, **1858**, 2778–2787.

Yoo, Y.J., **Lee, H.K.**, **Han, W.**, **Kim, D.H.**, **Lee, M.H.**, **Jeon, J.** ***et al.*** (2016) Interactions between transmembrane helices within monomers of the aquaporin AtPIP2;1 play a crucial role in tetramer formation. *Molecular Plant*, **9**, 1004–1017.

Yoshida, T., **Fujita, Y.**, **Sayama, H.**, **Kidokoro, S.**, **Maruyama, K.**, **Mizoi, J.** ***et al.*** (2010) AREB1, AREB2, and ABF3 are master transcription factors that cooperatively regulate ABRE-dependent ABA signaling involved in drought stress tolerance and require ABA for full activation. *The Plant Journal*, **61**, 672–685.

Yunta, C., **Martinez-Ripoll, M.**, **Zhu, J.K.** & **Albert, A.** (2011) The structure of Arabidopsis thaliana OST1 provides insights into the kinase regulation mechanism in response to osmotic stress. *Journal of Molecular Biology*, **414**, 135–144.

Zhu, J.K. (2016) Abiotic stress signaling and responses in plants. *Cell*, **167**, 313–324.